

Radiation Physics and Engineering 2021; 2(3):9–15

<https://doi.org/10.22034/rpe.2021.300458.1037>

Second order average current nodal expansion method for time-dependent neutron diffusion simulation

Kambiz Valavi, Ali Pazirandeh*, Gholamreza Jahanfarnia

Department of Nuclear Engineering, Science and Research Branch, Islamic Azad University, Tehran, Iran

HIGHLIGHTS

- Investigation of second order of average current nodal expansion method.
- Comparing zeroth and second order solution results.
- Perform static and dynamic calculation for each test case and compare the results with reference.

ABSTRACT

In the present work, a time-dependent neutron diffusion simulator is developed utilizing the second order of average current nodal expansion method. Generally, nodal methods can accurately simulate the reactor core with coarse meshes as long as the sizes of a fuel assembly. In this case, an adopted iterative approach is used for resolving the time-dependent three-dimensional multi-group neutron balance equations coupled with six-group precursor equations. In order to evaluate the implemented methodology, two popular transient problems are used including TWIGL two-dimensional seed-blanket reactor and three-dimensional LMW LWR. For indicating the precision of the method, the numerical results of high (second) order approach also have been compared with the basic methodology i.e. the zeroth order solution. From the comparison of obtained results with references, the suitable and precise simulating of transient schemes can be comprehended using the time-dependent second order average current nodal expansion method. Moreover, the results confirm that the second order solution can treat the coarse mesh kinetic problems with more accuracy relative to the basic approach.

KEYWORDS

Nodal expansion method
Neutron diffusion equation
Transient treatment
Precursor equations

HISTORY

Received: 19 August 2021
Revised: 21 September 2021
Accepted: 7 October 2021
Published: Summer 2021

1 Introduction

The spatial power distribution is a fundamental property for designing and analyzing the nuclear reactors. Answering the safety questions which arise in conjunction with actual or hypothetical accidental scenarios, often require the knowledge of multi-dimensional transient power distributions (Smith, 1979; Gehin, 1992).

In order to obtain the space-time dependent neutron flux distribution in the reactor core, one can employ the diffusion equation. In this respect, nodal method is one of methods which have been used for resolving the time-dependent neutron balance equation. In nodal methods, the neutron balance is preserved in each node (mesh). The merit of nodal methods, which preserve the neutron balance in each node (mesh), is the ability to model the geometry by coarse meshes with the sizes of a fuel assembly. As a result, nodal methods can be employed to solve problems that are computationally expensive, such as transient sim-

ulations in the reactor core. The analytical nodal method (ANM) (Smith, 1979) and the nodal expansion method (NEM) (Putney, 1986) can be noted as two of the popular nodal methods. The difference between these two methods is that, the ANM solves the neutron diffusion equation analytically but, in the NEM, this equation is treated by defining a linear polynomial expansion. In this regard, recently a computational simulator has been developed utilizing the second order average current nodal expansion method (ACNEM) for the three-dimensional rectangular geometry (Poursalehi et al., 2013). Also, in the other study, the results of the same static methodology for the three-dimensional hexagonal geometry have been presented (Poursalehi et al., 2014). Furthermore, a calculator code based on the flux expansion nodal method for the hexagonal lattice neutronic calculations of nuclear reactor has been employed (Mohammadnia et al., 2013). The nodal expansion method has been also developed for the neutron noise simulation described in some published

*Corresponding author: paziran@ut.ac.ir

works (Poursalehi et al., 2014; Abed et al., 2017; Poursalehi and Abed, 2021; Abed and Poursalehi, 2018).

Some methods also have been used for discretizing the time differential term in the time-dependent neutron balance equation in the literature, as well. For example, the backward difference formulas which have been utilized in standard methods (Ginestar et al., 1998) should resolve a large system of linear equations in any time step of the transient. Up to now, some papers have reported methods for simulating transients in the nuclear reactors core utilizing implicit methods (Hageman and Yasinsky, 1969), and applying the quasi-static method (Gehin, 1992), and by solving the fractional-space neutron point kinetics (F-SNPK) equations (Espinosa-Paredes, 2017).

In the present work, the time-dependent neutron balance equation coupled with precursors equations are solved using the second order of ACNEM. To resolve the time-dependent neutron diffusion equations, we have developed a new iterative method, which was proposed before for the steady-state treatment using ACNEM (Poursalehi et al., 2013, 2014). We also employ a fully implicit backward Euler approach, for discretizing the time differential terms of diffusion equations. It should be mentioned that the zeroth order ACNEM has been developed earlier for the transient calculations in the previous work (Valavi et al., 2020). In the current work, the results of second order ACNEM are also compared with the zeroth order results for time-dependent calculations. Two transient test cases including 2D seed-blanket reactor and 3D LMW LWR are simulated and investigated in order to validate the developed higher order approach. Results of both static and kinetic treatments prove the acceptable performance and the accuracy of the applied method in simulating the steady-state and transient schemes.

2 The static and kinetic calculations

In this section, the static and kinetic calculations of the second order ACNEM is explained, as a generalization of the zeroth order ACNEM, employed in Ref. (Valavi et al., 2020).

2.1 The static calculation using the second order average current nodal expansion method

The applied methodology for two-dimensional (2D) diffusion equation is briefly presented in this section which for 3D case, the method is similar. The 2D multi-group neutron continuity equation for node m is (Putney, 1986):

$$\sum_{\substack{u=x,y \\ s=l,r}} \frac{1}{h_u^m} \{j_{gus}^{+m} - j_{gus}^{-m}\} + \sum_{rg} \Phi_g^m = \sum_{\substack{g'=1 \\ g' \neq g}}^G \sum_{gg'} \Phi_{g'}^m + \frac{\chi_g}{k_{\text{eff}}} \sum_{g'=1}^G \nu \Sigma_{fg'}^m \Phi_{g'}^m \quad (1)$$

where $m = 1, 2, \dots, M$, $g = 1, 2, \dots, G$, and $u = x, y$. Also, j_{gus}^{+m} and j_{gus}^{-m} are the average outgoing (+) and incoming (−) partial currents for group g at the node surface of Γ_{us}^m ,

respectively. Φ_g^m is the average flux for group g in Π^m and h_u^m is the thickness of node Π^m for the u direction.

In the average current nodal expansion method (ACNEM), the flux distribution is defined by a polynomial expansion for each node and energy group. For the zeroth order version of ACNEM, as mentioned in previous work (Valavi et al., 2020), a second degree polynomial expansion, Eq. (2), is used as follows:

$$\Phi_g(x, y) = A_g h_0 + a_{gx} h_1(x) + b_{gx} h_2(x) + a_{gy} h_1(y) + b_{gy} h_2(y) + c_g h_1(x) h_1(y) \quad (2)$$

where $h_0 = 1$, $h_1(u) = u$, $h_2(u) = u^2 - \frac{1}{12}$, and $u = x, y$. The parameters of A_g , a_{gu} , and b_{gu} are obtained based on the values of the average flux, Φ_g^m , and the surface fluxes, Ψ_{gus}^m (Valavi et al., 2020). However, for the higher order of ACNEM, we consider the nodal expansion of Eq. (3) for Π^m node and energy group g by the below form:

$$\Phi_g^{[n]} = \Phi_g^{[0]} + \sum_{\substack{i=3 \\ u=x,y}}^{n+2} d_{gui-2} h_i(u) + \sum_{\substack{i+j \leq n+2 \\ i,j=1 \\ i+j \neq 2}} c_{gij} h_i(x) h_j(y) \quad ; \quad n \geq 1 \quad (3)$$

where $\Phi_g^{[0]}$ is the zeroth order expansion (2), and $h_i(u)$ is a polynomial expansion of degree i in the u direction. Here n and $n + 2$ represent the order and degree of the expansion, respectively.

Due to the orthogonality properties of the expansion functions, the weighted residual form of Eq. (1) splits into a pair of independent one dimensional weighted diffusion equation, i.e.:

$$\int_{-\frac{h_u^m}{2}}^{\frac{h_u^m}{2}} W_k(u) \left\{ -D_g^m \frac{d^2 \Psi_{gu}^m}{d^2 u} + \Sigma_{rg} \Psi_{gu}^m + L_{gu}^m - \sum_{\substack{g'=1 \\ g' \neq g}}^G \Sigma_{gg'}^m \Psi_{g'u}^m - \frac{\chi_g}{k_{\text{eff}}} \sum_{g'=1}^G \nu \Sigma_{fg'}^m \Psi_{g'u}^m \right\} du = 0 \quad (4)$$

where $m = 1, 2, \dots, M$, $g = 1, 2, \dots, G$, $u = x, y$, and

$$\Psi_{gu}^m = \frac{1}{h_v^m} \int_{-\frac{h_v^m}{2}}^{\frac{h_v^m}{2}} \Phi_g^m dv \quad ; \quad u = x, y, \quad v \neq u \quad (5)$$

is the one-dimensional spatially averaged flux for the u -direction and L_{gu}^m is the u -dependent transverse leakage.

With the transverse leakage moments at hand, the weighted residual Eq. (4) can be evaluated. The equations for the 1st and 2nd order expansion coefficients (d_{gu1} , d_{gu2})

in the u -direction are resulted as the following relations:

$$\begin{aligned} & \left\{ \frac{D_g^m}{h_u^{m^2}} + A_k \Sigma_{rg}^m \right\} d_{guk}^m \\ &= \sum_{\substack{g'=1 \\ g' \neq g}}^G \Sigma_{gg'}^m \left\{ A_k d_{g'uk}^m - B_k e_{g'uk}^m \right\} \\ &+ \frac{\chi_g}{k_{\text{eff}}} \sum_{g'=1}^G \nu \Sigma_{fg'}^m \left\{ A_k d_{g'uk}^m - B_k e_{guk}^m \right\} \\ &+ B_k \Sigma_{rg}^m e_{guk}^m + B_k L_{guk}^m \end{aligned} \quad (6)$$

where $m = 1, 2, \dots, M$, $g = 1, 2, \dots, G$, $k = 1, 2$, $u = x, y$, and A_k and B_k are constant coefficients. Also, e_{gu1}^m and e_{gu2}^m are the zeroth order expansion coefficients, i.e. a_{gu} and b_{gu} , respectively (Poursalehi et al., 2013; Valavi et al., 2020).

Additional relations using the average surface partial currents ($j_{gus}^{+m}, j_{gus}^{-m}$) are required for solving Eq. (1). A set of equations is employed for relating the outgoing currents to the incoming currents and the average flux in each node and energy group. The interface current equations are derived as (Valavi et al., 2020):

$$\begin{bmatrix} j_{gul}^{+m} \\ j_{gur}^{+m} \end{bmatrix} = \begin{bmatrix} A_{gu}^m & B_{gu}^m & C_{gu}^m & -D_{gu}^m & E_{gu}^m \\ A_{gu}^m & C_{gu}^m & B_{gu}^m & D_{gu}^m & E_{gu}^m \end{bmatrix} \begin{bmatrix} \Phi_g^m \\ j_{gul}^{-m} \\ j_{gur}^{-m} \\ d_{gu1}^m \\ d_{gu2}^m \end{bmatrix} \quad (7)$$

where $m = 1, 2, \dots, M$, $g = 1, 2, \dots, G$, and $u = x, y$. Also, the nodal coefficients $A_{gu}^m - E_{gu}^m$ are rational functions of $\frac{D_g^m}{h_u^m}$.

Finally, by employing Eq. (7) and eliminating the outgoing currents from Eq. (1), Eq. (8) is derived for calculating the average fluxes in nodes (Valavi et al., 2020):

$$\begin{aligned} & \left[\sum_{u=x,y} 2 \frac{A_{gu}^m}{h_u^m} + \Sigma_{rg}^m \right] \Phi_g^m = \sum_{\substack{g'=1 \\ g' \neq g}}^G \Sigma_{gg'}^m \Phi_{g'}^m \\ &+ \frac{\chi_g}{k_{\text{eff}}} \sum_{g'=1}^G \nu \Sigma_{fg'}^m \Phi_{g'}^m \\ &+ \sum_{u=x,y} \frac{1}{h_u^m} \left\{ (1 - B_{gu}^m - C_{gu}^m) \times \right. \\ & \left. (j_{gul}^{-m} - j_{gur}^{-m}) - 2E_{gu}^m d_{gu2}^m \right\} \end{aligned} \quad (8)$$

where $m = 1, 2, \dots, M$, $g = 1, 2, \dots, G$, and $u = x, y$.

In order to obtain the required unknown nodal parameters, Eqs. (6) to (8) are solved simultaneously along with implementing the continuity of interface currents for neighbor nodes and boundary conditions for exterior nodes. The iterative algorithm for treating the above equations has been described in (Poursalehi et al., 2013; Valavi et al., 2020).

2.2 The kinetic calculation using the second order average current nodal expansion method

For simulating transient scenarios in nuclear reactors core, the time-dependent solution of diffusion equation can be performed employing the second order ACNEM.

The time-dependent form of Eq. (1) by using the implicit approach of the backward Euler method is presented in Eq. (9) for the time t and energy group g (Valavi et al., 2020; Christensen, 1985):

$$\begin{aligned} \Phi_g^m(t) &= \Phi_g^m(t - \Delta t) + v_g \Delta t \cdot \left(\sum_{u=x,y} \frac{1}{h_u^m} \times \right. \\ & \left\{ (1 - B_{gu}^m(t) - C_{gu}^m(t)) (j_{gul}^{-m}(t) + j_{gur}^{-m}(t)) \right. \\ & \left. - 2E_{gu}^m(t) d_{gu2}^m(t) \right\} - \left[\sum_{u=x,y} 2 \frac{A_{gu}^m(t)}{h_u^m} \right. \\ & \left. + \Sigma_{rg}^m(t) \right] \Phi_g^m(t) + \sum_{\substack{g'=1 \\ g' \neq g}}^G \Sigma_{gg'}^m(t) \Phi_{g'}^m(t) \\ &+ \sum_{g'=1}^G (1 - \beta) \frac{\chi_{pg'}}{k_{\text{eff}}} \nu \Sigma_{fg'}^m(t) \Phi_{g'}^m(t) \\ &+ \sum_{i=1}^I \lambda_i \chi_{dg}^i c_i^m(t) \end{aligned} \quad (9)$$

Here, χ_{pg} and χ_{dg} are the emission spectrum of prompt and delayed neutrons for group g , β is the total fraction of delayed neutrons, λ_i and c_i are the decay constant and concentration of the i^{th} delayed neutron family, and v_g is the neutron velocity for energy group g .

Also, for calculating the time-dependent concentrations of delayed neutron emitters, $c_i^m(t)$, the volume integrated form of precursor equations (Christensen, 1985) are considered as:

$$\begin{aligned} c_i^m(t) &= \frac{1}{(1 + \lambda_i \Delta t)} \left(c_i^m(t - \Delta t) + \Delta t \frac{1}{k_{\text{eff}}} \beta_i \right. \\ & \left. \times \sum_{g'=1}^G \nu \Sigma_{fg'}^m(t) \Phi_{g'}^m(t) \right) \end{aligned} \quad (10)$$

where $m = 1, 2, \dots, M$, and $i = 1, 2, \dots, I$. Also, β_i is the delayed neutron fraction of the i^{th} delayed neutron family and I is the number of delayed neutron families. As represented in Eq. (9), the 1st and 2nd order expansion coefficients should be calculated for each time step. The equations for obtaining the time-dependent high order expansion coefficients in the u -direction are shown in the followings:

Table 1: The comparison of static results for the TWIGL SEED-BLANKET-2D reactor problem.

	k_{eff}^*	k_{eff}	Relative Error (%)	Max. Power Rel. Error (%)	Ave. Power Rel. Error (%)
Zerth Order	0.91276		-0.046	4.69	1.68
Second Order	0.91320		0.002	1.33	0.12

* k_{eff} (reference): 0.91318

$$\begin{aligned}
& \left\{ \frac{D_g^m(t)}{h_u^m} + A_k \Sigma_{rg}^m(t) + A_k \frac{\Phi_g^m(t) - \Phi_g^m(t - \Delta t)}{\Delta t \cdot v_g} \right\} \\
& \times d_{guk}^m(t) = \sum_{\substack{g'=1 \\ g' \neq g}}^G \Sigma_{gg'}^m(t) \left\{ A_k d_{g'uk}^m(t) - B_k e_{g'uk}^m(t) \right\} \\
& + \frac{(1 - \beta) \chi_g}{k_{\text{eff}}} \sum_{g'=1}^G \nu \Sigma_{fg'}^m(t) \left\{ A_k d_{g'uk}^m(t) \right. \\
& \left. - B_k e_{g'uk}^m(t) \right\} + B_k \Sigma_{rg}^m(t) e_{guk}^m(t) + B_k L_{guk}^m(t) \\
& - B_k \frac{\sum_{g'=1}^G e_{g'uk}^m(t)}{\sum_{g'=1}^G \Phi_{g'}^m(t)} \sum_{i=1}^I \lambda_i \chi_{dg}^i c_i^m(t)
\end{aligned} \quad (11)$$

where $m = 1, 2, \dots, M$, $g = 1, 2, \dots, G$, $k = 1, 2$, and $u = x, y$. Also, A_k , B_k , and L_{guk}^m have the same definitions noted in the Ref (Valavi et al., 2020).

In order to resolve the coupled time-space dependent Eqs. (9) and (10), an adopted iterative approach has been developed using the second order ACNEM. The detailed time-dependent algorithm using ACNEM has been presented in our previous published paper (Valavi et al., 2020). Therefore, the respectable reader is referred to (Valavi et al., 2020) for more information.

3 Numerical Results

For evaluating the proposed approach, numerical results of two transient problems including TWIGL 2D seed-blanket reactor and 3D LMW LWR are presented in this section and compared with references for both static and kinetic simulations.

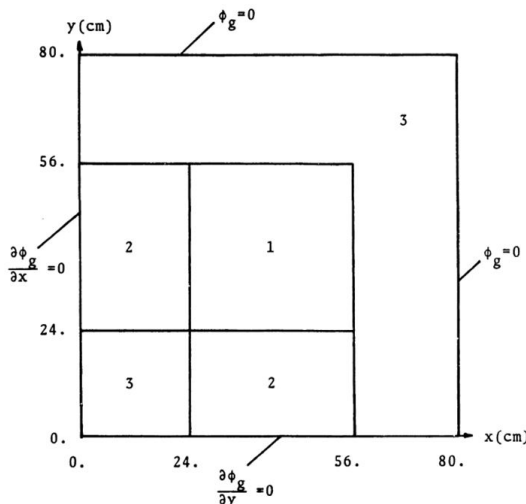


Figure 1: Quadrant of TWIGL seed-blanket reactor core (Smith, 1979).

3.1 TWIGL seed-blanket reactor problem

The first test case (Valavi et al., 2020) named TWIGL seed-blanket reactor problem is a 2D model of a 160 cm square un-reflected seed-blanket reactor. This case has the eighth symmetry of core and is specified by two neutron energy groups. For this test case, transient solutions have been presented firstly by (Hageman and Yasinsky, 1969) and investigated later in some papers such as (Smith, 1979; Christensen, 1985). Figure 1 illustrates the geometry dedicated to the TWIGL problem (Christensen, 1985). The steady-state treatment of the TWIGL problem has been done using the second order ACNEM. In this procedure, coarse meshes have been considered with the sizes of 8×8 cm². The reference for this problem is the second order solution of ACNEM given in (Christensen, 1985). The obtained numerical results of the zeroth and second order solutions and their relative errors in comparison to the reference are exhibited in Table 1. According to this table, the accurate treatment of the steady-state multi-group diffusion equation is apprehended using nodal approaches, specifically the second order solution.

For the time-dependent calculation, two different transients are defined. These schemes are initiated in region 1 by decreasing the thermal absorption cross section including the step perturbation, i.e.:

$$\Delta \Sigma_{a_2} = -0.0035 \text{ cm}^{-1}; \quad t = 0 \quad (12)$$

And the ramp perturbation in 0.2 s as (Christensen, 1985):

$$\Sigma_{a_2}(t) = \begin{cases} \Sigma_{a_2}(0)(1 - 0.11667t); & t \leq 0.2 \\ \Sigma_{a_2}(0)(0.97666) & t > 0.2 \end{cases} \quad (13)$$

Both transients have been simulated by the developed time-dependent zeroth and second orders of ACNEM for 0.5 s with the time step length of 0.01 s. Therefore, 50 time steps are defined for the kinetic calculation. Moreover, the reference is the numerical results of the QUANDRY code for both transients (Christensen, 1985).

According to Eq. (12), the step perturbation has been implemented in the region 1 of the TWIGL seed-blanket reactor core and the results have been gained during the time, step by step. In this case, the relative average powers of the reactor core along the time earned by the second order ACNEM are compared by the reference in Table 2.

Moreover, Fig. 2 shows the relative average powers of the core versus the time belonging to the developed second order simulator. Also, the comparison of power relative errors of zeroth and second order solutions for time steps noted in Table 2 is indicated in Table 3. This table proves that the errors of results of the second order methodology are smaller relative to the zeroth order treatment for the step perturbation simulation in the core.

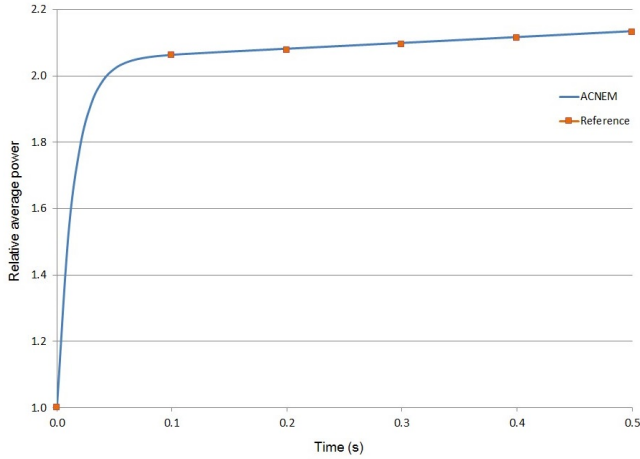


Figure 2: Relative average power along time for the step perturbation of TWIGL seed-blanket reactor.

Table 2: Relative average power along time for the step perturbation of the TWIGL SEED-BLANKET-2D reactor problem.

Time (s)	ACNEM ^{*,†}	Reference	Rel. Error (%)
0.00	1.000	1.000	-
0.05	2.022	-	-
0.10	2.064	2.061	0.13
0.15	2.073	-	-
0.20	2.082	2.078	0.20
0.25	2.091	-	-
0.30	2.100	2.095	0.22
0.35	2.108	-	-
0.40	2.117	2.113	0.20
0.45	2.126	-	-
0.50	2.135	2.131	0.19

* Time step length: 10^{-2} s

† For the second order solution

Table 3: Relative errors of average power for the step perturbation of the TWIGL SEED-BLANKET-2D reactor problem.

Order of Solution	Max. Power Rel. Error (%)	Ave. Power Rel. Error (%)
Zerth Order	-0.55	-0.51
Second Order	0.22	0.19

Table 4: Relative average power along time for the ramp perturbation of the TWIGL SEED-BLANKET-2D reactor problem.

Time (s)	ACNEM ^{*,†}	Reference	Rel. Error (%)
0.00	1.000	1.000	-
0.05	1.127	-	-
0.10	1.310	1.307	0.23
0.15	1.573	-	-
0.20	1.961	1.957	0.21
0.25	2.068	-	-
0.30	2.080	2.092	0.28
0.35	2.089	-	-
0.40	2.097	2.092	0.25
0.45	2.106	-	-
0.50	2.115	2.109	0.28

* Time step length: 10^{-2} s

† For the second order solution

According to Eq. (13), the ramp perturbation has been simulated with respect to time in the reactor core. Table 4 gives the values of relative average power obtained by the second order solution for some time instances and also their relative errors in comparison to the reference. In addition, Fig. 3 presents the values of relative average power for the second order treatment during the time for the ramp perturbation. Table 5 also presents the maximum and average of relative errors for both zeroth and second order calculations.

Table 5: Relative errors of average power for the ramp perturbation of the TWIGL SEED-BLANKET-2D reactor problem.

Order of Solution	Max. Power Rel. Error (%)	Ave. Power Rel. Error (%)
Zerth Order	-0.45	-0.40
Second Order	0.28	0.25

3.2 LMW LWR-3D problem

For the second problem (Valavi et al., 2020), a 3D reactor core called the LMW (Langenbuch-Maurer-Warner) test case is investigated. This reactor has a two-zone core including 77 fuel assemblies by widths of 20 cm. The core is reflected by 20 cm of water both radially and axially, and the height of active core is 160 cm. Schematic axial view of the LMW LWR-3D core is shown in Fig. 4 (Smith, 1979). The movements of two groups of control rods are considered as the transient for this test case which the initial and final positions of control rods are identified in Fig. 4. It should be noted that the calculations have been performed by ignoring the cusping effect treatment.

The developed simulator using the second order of ACNEM has been run for the quarter symmetry of LMW LWR-3D. In the steady-state modeling of LMW LWR, the initial position of the 1th group control rod is shown in Fig. 4. The problem has been modeled with 3D coarse meshes by the sizes of a fuel assembly i.e. $20 \times 20 \times 20$ cm³. The results of the QUANDRY code (Smith, 1979) with the mesh sizes of $10 \times 10 \times 10$ cm³ are also elected as the reference for both static and kinetic treatments. Table 6 represents the static parameters including the effective multiplication factor and its relative error, the maximum and average of fuel assembly power errors in comparison to the reference for both zeroth and second order solutions. Numerical results noted in Table 6 verify a suitable static modeling of the LMW LWR-3D particularly for the second order treatment.

In order to perform a time-dependent calculation, the following transient scheme is defined by moving the groups of control rods (Smith, 1979):

$$\begin{cases} \text{Removing rod group 1 at } 3.0 \text{ cm.s}^{-1}; & 0 \leq t \leq 26.666 \text{ s} \\ \text{Inserting rod group 2 at } 3.0 \text{ cm.s}^{-1}; & 7.5 \leq t \leq 47.5 \text{ s} \end{cases} \quad (14)$$

Table 6: The comparison of static results for the LMW LWR-3D reactor test case.

	k_{eff}^*	k_{eff} Relative Error (%)	Max. Power Rel. Error (%)	Ave. Power Rel. Error (%)
Zereth Order	1.00058	0.091	4.02	1.65
Second Order	0.99958	-0.008	-1.28	0.33

* k_{eff} (reference): 0.99966

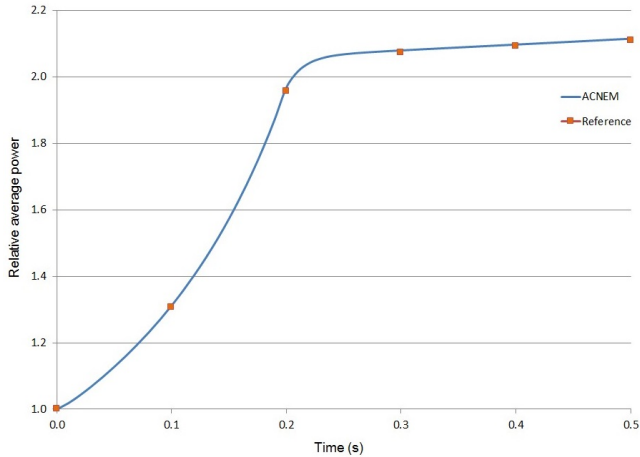


Figure 3: Relative average power along time for the ramp perturbation of TWIGL seed-blanket reactor.

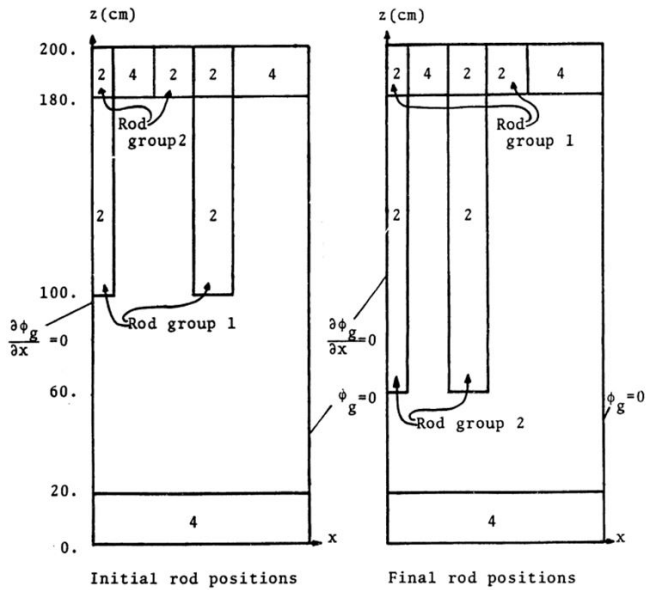


Figure 4: The schematic view of LMW LWR-3D in the axial direction (Smith, 1979).

The kinetic calculation has been fulfilled for 60 s, step by step, according to the perturbation strategy noted in Eq. (14). Moreover, the length of selected time step is 0.8 s. In this way, the time-dependent two energy-groups neutron diffusion equations coupled with the six-group delayed neutron equations have been resolved employing both the zeroth and second versions of ACNEM. For this purpose, the defined changes of corresponding cross-sections have been implemented in the simulator, step by step, as for the transient program which is given in Eq. (14). Table 7 reveals the relative average powers

in the reactor core gained by the second order simulator for some time steps which are compared with the reference (Smith, 1979). Fig. 5 also illustrates the schematic diagram of the relative average power variations along the time. According to Table 7 and Fig. 5, the appropriate accuracy of developed attitude, i.e. the time-dependent second order of ACNEM, is observed in comparison to the reference. At last, the maximum and average of relative errors of powers for the zeroth and second order calculations are given in Table 8. As represented in Table 8, the second order time-dependent nodal method can simulate the transient scheme by more accuracy in comparison to the basic approach, i.e. the zeroth order ACNEM when the coarse meshes, are employed.

Table 7: Relative average power along time for the LMW LWR-3D test case.

Time (s)	ACNEM ^{*,†}	Reference	Rel. Error (%)
0	1.000	1.000	-
5	1.132	1.114	1.61
10	1.341	1.313	2.13
15	1.568	-	-
20	1.664	1.669	-0.30
25	1.545	-	-
30	1.332	1.340	-0.60
35	0.987	-	-
40	0.766	0.793	-3.40
45	0.575	-	-
50	0.480	0.494	-2.83
55	0.415	-	-
60	0.369	0.379	-2.64

* Time step length: 0.8 s

† For the second order solution

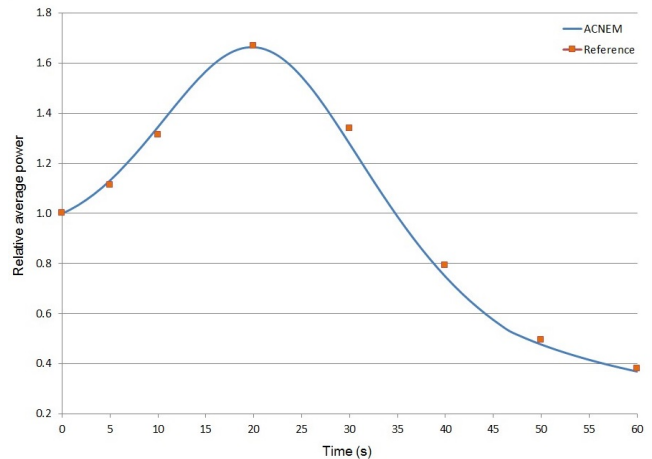


Figure 5: Relative average power along time for the LMW LWR-3D.

Table 8: Relative errors of average power for the LMW LWR-3D reactor problem.

Order of Solution	Max. Power	Ave. Power
	Rel. Error (%)	Rel. Error (%)
Zeroth Order	-5.1	2.6
Second Order	-3.4	1.9

4 Conclusion

In this work, the time-dependent treatment of neutron balance equation has been performed utilizing the second order of ACNEM. To do so, an adapted iterative approach has been used for simulating the transient schemes in nuclear reactors. For evaluating the proposed approach, two well-known transient problems have been modeled exploiting coarse meshes with the sizes of a fuel assembly. For representing the proper modeling of transients using the implemented method, results of both static and kinetic calculations have been compared with the results of authentic references. Our results show that the developed coarse mesh simulator using the second order of ACNEM can resolve precisely the transient problems of nuclear reactors core. Moreover, for indicating the power of the second order ACNEM to model the transients using coarse meshes, the zeroth order version of ACNEM has also been developed. According to the results, the second order treatment can simulate the coarse mesh time-dependent problems by more precision in comparison to the zeroth order solution. The results confirm that the numerical errors can be decreased significantly utilizing the second order treatment relative to the basic version for the coarse mesh calculations.

References

- Abed, A. and Poursalehi, N. (2018). Neutron noise simulation in the nuclear reactor core based on the average current nodal expansion method. *Annals of Nuclear Energy*, 114:482–494.
- Abed, A., Poursalehi, N., and Zolfaghari, A. (2017). Point flux nodal expansion scheme applied to the neutron noise analysis of the nuclear reactor core. *Progress in Nuclear Energy*, 94:133–146.
- Christensen, B. (1985). Three-dimensional static and dynamic reactor calculations by the nodal expansion method.
- Espinosa-Paredes, G. (2017). Fractional-space neutron point kinetics (F-SNPK) equations for nuclear reactor dynamics. *Annals of Nuclear Energy*, 107:136–143.
- Gehin, J. C. (1992). A quasi-static polynomial nodal method for nuclear reactor analysis. Technical report, Oak Ridge Inst. for Science and Education, TN (United States); Massachusetts .
- Ginestar, D., Verdú, G., Vidal, V., et al. (1998). High order backward discretization of the neutron diffusion equation. *Annals of Nuclear Energy*, 25(1-3):47–64.
- Hageman, L. and Yasinsky, J. (1969). Comparison of alternating-direction time-differencing methods with other implicit methods for the solution of the neutron group-diffusion equations. *Nuclear Science and Engineering*, 38(1):8–32.
- Mohammadnia, M., Pazirandeh, A., and Sedighi, M. (2013). Development of a computer code for neutronic calculations of a hexagonal lattice of nuclear reactor using the flux expansion nodal method. *Nuclear Technology and Radiation Protection*, 28(3):237–246.
- Poursalehi, N. and Abed, A. (2021). Second order of average current nodal expansion method for the neutron noise simulation. *Nuclear Engineering and Technology*, 53(5):1391–1402.
- Poursalehi, N., Zolfaghari, A., and Minuchehr, A. (2013). Development of a high order and multi-dimensional nodal code, ACNEC3D, for reactor core analysis. *Annals of Nuclear Energy*, 55:211–224.
- Poursalehi, N., Zolfaghari, A., and Minuchehr, A. (2014). Three-dimensional high order nodal code, ACNECH, for the neutronic modeling of hexagonal-z geometry. *Annals of Nuclear Energy*, 68:172–182.
- Putney, J. (1986). A hexagonal geometry nodal expansion method for fast reactor calculations. *Progress in Nuclear Energy*, 18(1-2):113–121.
- Smith, K. S. (1979). *An analytic nodal method for solving the two-group, multidimensional, static and transient neutron diffusion equations*. PhD thesis, Massachusetts Institute of Technology.
- Valavi, K., Pazirandeh, A., and Jahanfarnia, G. (2020). Three-dimensional time-dependent neutron diffusion simulation using average current nodal expansion method. *Nuclear Technology and Radiation Protection*, 35(3):189–200.